

## Polythiophene/TiO<sub>2</sub> and polythiophene/ZrO<sub>2</sub> nanocomposites: physical and antimicrobial properties against common infections

Sina Khanmohammadi<sup>1,2</sup>, Ramin Karimian<sup>3,\*</sup>, Farid Hajibonabi<sup>2</sup>, Elmira Mostafidi<sup>4</sup>, Asghar Tanomand<sup>5</sup>, Ladan Edjlali<sup>6</sup>, Zahra Khalili Azami<sup>7</sup>, Mojtaba Ghanbari Mehrabani<sup>1</sup>, Hossein Samadi Kafil<sup>1,\*</sup>

<sup>1</sup>Drug Applied Research Center, Tabriz University of Medical Sciences, Tabriz, Iran

<sup>2</sup>Student Research Committee, Tabriz University of Medical Sciences, Tabriz, Iran

<sup>3</sup>Chemical Injuries Research Center, Systems biology and poisonings institute, Baqiyatallah University of Medical Sciences, Tehran, Iran

<sup>4</sup>Connective Tissue Diseases Research Center, Tabriz University of Medical Sciences, Tabriz, Iran

<sup>5</sup>Department of Microbiology, Maragheh University of Medical Sciences, Maragheh, Iran.

<sup>6</sup>Department of Chemistry, Islamic Azad University, Tabriz Branch, Tabriz, Iran.

<sup>7</sup>Department of Chemical Engineering, Malek Ashtar University, Tehran, Iran.

\*corresponding author e-mail address: karimian.r@gmail.com, kafilhs@tbzmed.ac.ir

### ABSTRACT

The development of nanotechnology enables the provision of optimal and useful materials in various fields, including polymer nanocomposites. By using metal oxide nanostructures produce metallic oxide nanocomposites which are widely used in various industries. In this study, polythiophene/TiO<sub>2</sub> and polythiophene/ZrO<sub>2</sub> nanocomposites were synthesized and the properties of nanocomposites were characterized using various techniques such as FT-IR, XRD, TGA and SEM analysis to obtain the exact structure of nanocomposites. The results showed thermal strength and stability for the prepared nanocomposites which the polythiophene/TiO<sub>2</sub> nanocomposite has more thermal stability compared to polythiophene/ZrO<sub>2</sub>. The analysis of the XRD showed that the crystalline structures of TiO<sub>2</sub> and ZrO<sub>2</sub> in the nanocomposite were changed by polythiophene. Besides, polythiophene/TiO<sub>2</sub> nanocomposite had higher antibacterial properties compared to polythiophene/ZrO<sub>2</sub> against *E.coli* bacteria, but polythiophene/ZrO<sub>2</sub> nanocomposite had a better effect against *S. aureus*. In addition, the two nanocomposites prepared in this study had less antifungal activity compared with their antibacterial properties.

**Keywords:** Nanocomposite, polythiophene/TiO<sub>2</sub>, polythiophene/ZrO<sub>2</sub>, and antimicrobial activity.

### 1. INTRODUCTION

Nowadays, with the rapid development of nanotechnology, the possibility of the efficient preparation and use of polymer nanocomposites is widely available (1, 2). In recent years, the focus of research and scientific studies are simultaneously using the properties of the semiconductor polymers, as well as the properties of metal oxides for the production of new polymer nanocomposites that have better physical and chemical property (2-5). Nanostructured metal oxides have attracted the attention of many researchers with unique optical(1), electronic(6), and magnetic properties(2), low cost, and eco-friendly properties(3, 7). Due to its unique chemical and physical properties such as high strength, chemical stability, high resistance to corrosion and microbial and chemical agents, Zirconium has always been considered by the researchers (8, 9). Zirconium dioxide and titanium dioxide are the most important transition metal oxides, which are used in many fields such as oxygen sensors, optical coatings, electro ceramic, fuel cells, electrochemical devices(10), catalysts and dielectrics (9). With the rapid development of nanotechnology, polymer nanocomposites containing nanoparticles were rapidly expanding (9, 11). In recent years, many researchers have come up with new polymer nanocomposites using metal oxide nanoparticles that create unique physical and chemical properties (7, 12, 13). In the research, experimental parameters such as polymerization methods,

temperature, solvent, and oxidant type used in the preparation of nanocomposites have been considered, because these factors play a very important role in determining the optimal chemical and microbial properties of these (14-16). In recent years, various types of polythiophene nanocomposites have been prepared with various metal oxides. Guo et al. showed that polythiophene/vanadium lithium oxide nanocomposite can be used in lithium ion batteries (17). Also, Huang et al. showed that the polythiophene/ WO<sub>3</sub> nanocomposite can be used as a gas sensor component to detect low levels of NO<sub>2</sub> at low temperatures (18). Zhu et al. found that the polythiophene / ZrO<sub>2</sub> nanocomposite exhibits high photocatalytic activity (19). Dongmei et al. produced polythiophene/ZrO<sub>2</sub> nanocomposite films using a sol-gel method (20).

In this study, ZnO<sub>2</sub> and TiO<sub>2</sub> oxide nanoparticles have been considered and polythiophene polymer has been selected. Polythiophene was considered for its high thermal, chemical and environmental sustainability(21, 22). This feature has made it a lot of uses in the production of solar cells, electrical equipment and sensors (18-20). Different identification methods such as FT-IR, XRD, TGA, and SEM have been used to determine the properties of nanocomposites in order to determine the exact structure of prepared nanocomposite. Also, the anti-bacterial properties of nanocomposites for *E. coli* were determined.

## 2. EXPERIMENTAL SECTION

**2.1. Materials and Methods.** In the present study, thiophene and ferric chloride ( $\text{FeCl}_3$ ) (as the starting material for the polymerization process), chloroform ( $\text{CHCl}_3$ ), and methanol ( $\text{CH}_3\text{OH}$ ) were purchased from Merck Company. Thiophene monomers were distilled under reduced pressure before use. The  $\text{TiO}_2$  and  $\text{ZrO}_2$  nanoparticles (NPs) were purchased from US Research Company. For dehydration of chloroform as a solvent in the polymerization process of thiophene following procedure was done before the examination. Firstly, 250 mL of  $\text{CHCl}_3$  and 5 g of  $\text{CaCl}_2$  are poured into the round bottom flask and stirred for an overnight. Then, the purification of chloroform from impurities such as  $\text{CaCl}_2$  was done according to standard purification method.

**2.2. Characterizations.** Fourier-transform infrared (FTIR) spectroscopy was used to analyze the structure and determination of sample's functional groups. FTIR spectra were recorded on a Bruker (Shimadzu, Japan) by KBr method and scanned against a blank KBr disk at wavenumbers ranging from 400 to 4000  $\text{cm}^{-1}$ . The size and morphology of samples were determined using a scanning electron microscopy (FESEM-EDX; TESCAN 5001). Before analysis, samples were mounted onto a metal stub using a carbon double-sided adhesive tape, and covered with a thin layer of gold, with the aid of a direct current sputter technique (Emitechk 450X, England). Powder X-ray diffraction patterns of the samples were recorded on a Bruker AXS model D8 Advance Diffractometer using  $\text{CuK}\alpha$  radiation ( $\lambda=1.542\text{\AA}$ ), with the Bragg angle ranging from  $2\theta=10-80^\circ$ .

**2.3. Preparation of polythiophene.** The pure polythiophene was prepared by a chemical oxidation polymerization method according to the literature with slight modification (Fig. 1A) (23). In brief, in a round bottom flask equipped with reflux condenser and dropping funnel, 1 mL (12.73 mmol) of distilled thiophene as a monomer was dissolved in 40 mL of dried chloroform and stirred moderately for 10 min. Then, 15 ml of dry  $\text{CHCl}_3$  containing  $\text{FeCl}_3$  (8.26 g; 12.73 mmol) as an oxidizing agent was added gradually into the reaction mixture via dropping funnel. This reaction process was carried out at reflux temperature under an inert atmosphere. By observing color changes in the solvent from white to dark, it was found that the polymerization was started and completed. When the color of the solution was altered to the completely black, it was shown that the polymerization reaction stopped. The resulting black polymer was poured in 100 mL of methanol to extract the polymer from chloroform. By staining the methanol polymer for 24 hours, the color of the product changes from black to red. To remove  $\text{FeCl}_3$  from the

polymer, the washing process is carried out using filter paper. The synthesized polymer was dried in the vacuum oven at 60  $^\circ\text{C}$  for 24 h. After rubbing and crushing of product, the prepared powder was kept in the sterilized container for further uses.

**2.4. Preparation of polythiophene/ $\text{TiO}_2$  and polythiophene/ $\text{ZrO}_2$  nanocomposites.** Three different amounts of  $\text{TiO}_2$  or  $\text{ZrO}_2$  NPs (0.05, 0.10, and 0.20 g) were suspended in 40 mL of dried chloroform via probe-type ultrasonic for 30 min. Subsequently, 1 mL distilled thiophene as a monomer was added to the above suspension and stirred for 20 min to obtain a homogenous suspension. Then, 20 mL  $\text{FeCl}_3$  solution in dry chloroform containing 8.26 g  $\text{FeCl}_3$  was added the suspension drop by drop and stirred continuously at reflux temperature via magnetic stirrer. The polymerization process was started immediately which reaction mixture color was changed from white to dark in 24 h. Finally, the black polymer was collected using filter paper and washed several times with distilled water and methanol. Polythiophene/ $\text{TiO}_2$  and polythiophene/ $\text{ZrO}_2$  nanocomposites were prepared with the different amount of NPs which named as 0.05, 0.10, 0.20 nanocomposites.

**2.5. Antimicrobial assays.** Antimicrobial properties were evaluated by Kerby Bauer method according to Clinical laboratory standard Institute (CLSI) protocol (24, 25). Three standard strains including *Staphylococcus aureus* ATCC<sup>®</sup> 25923<sup>™</sup> as Gram-positive pathogen, *Escherichia coli* ATCC<sup>®</sup> 25923<sup>™</sup> as Gram-negative pathogen and *Candida albicans* (Robin) Berkhout (ATCC<sup>®</sup> 10231<sup>™</sup>) were used in this study. These are recommended strains by CLSI for evaluating antimicrobial properties. Muller-Hinton Agar (Merck, Germany) and Muller-Hinton Agar plus 1% glucose (for fungi) were used for analysis (26). pH of Muller-Hinton Agar should be adjusted between 7.2-7.4 that it is used. All pathogens were subcultured for 24h and then used for the study. Microbial cultures were adjusted with turbidity equal to 0.5 Mc Farland (density of a microbial suspension with  $1.5 \times 10^8$  colony forming units (CFU/ml)). After microbes have been inoculated for a maximum of 15 min, Polythiophene/ $\text{TiO}_2$  and polythiophene/ $\text{ZrO}_2$  nanocomposites should be placed at the center of agar culture with an appropriate distance from borders. Then plates were kept for 18h at 35  $^\circ\text{C}$  in an incubator. Inhibition zone for each microbe was measured by a ruler. The gentamicin(10 $\mu\text{l}$ ), Flocunazole (25 $\mu\text{l}$ ) and Dimethyl sulfoxide (DMSO) discs were used as positive control for bacteria, fungi, and negative control respectively. All experiments were done in triplicate.

## 3. RESULTS SECTION

**3.1. Preparation of nanocomposites.** In the present work, we are endeavoring to develop the  $\text{TiO}_2$  and  $\text{ZrO}_2$  nanocomposites based on polythiophene. The synthetic route for the preparation of pure polythiophene and polythiophene nanocomposites were illustrated in Fig. 1. A-B. Firstly, pure polythiophene was synthesized

according to the published procedures as described in the experimental section. In order to obtain nanocomposites, polythiophene was prepared in  $\text{TiO}_2$  and  $\text{ZrO}_2$  nanoparticles (NPs) suspension in presence of ferric chloride ( $\text{FeCl}_3$ ) as an oxidizing agent. Two kinds of nanocomposite were obtained based on

polythiophene polymeric platform. Finally, the prepared nanocomposites were characterized and used in the further antimicrobial activity.

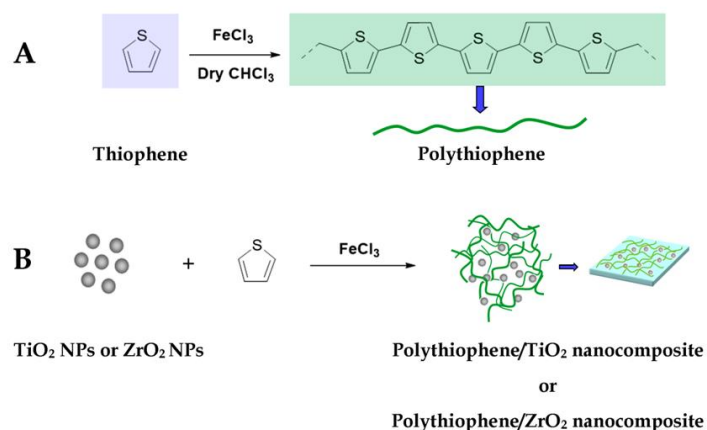


**Fig. 1.** The synthetic route for the preparation of polythiophene (A) and polythiophene/TiO<sub>2</sub> and polythiophene/ZrO<sub>2</sub> nanocomposites (B).

**3.2. Characterization of nanocomposites.** The FT-IR spectra of TiO<sub>2</sub> nanocomposite and starting materials were obtained using KBr disks in the range of 400-4000 cm<sup>-1</sup> (Fig. 2). In pure TiO<sub>2</sub>, an original peak at 585 cm<sup>-1</sup> and a weak peak at 1104 cm<sup>-1</sup> were observed. The peak obtained in 585 cm<sup>-1</sup> corresponds to an octahedral absorption peak [TiO<sub>6</sub>]. A peak at 1644 cm<sup>-1</sup> is related to C = C thiophene which is in the fingerprint area. The absorption peak at 795 cm<sup>-1</sup> relates to the tensile vibration of the C-H outside the plate of the thiophene ring. The absorption of 697 cm<sup>-1</sup> corresponds to the C-S bond, which is the presence of thiophene monomer in the polymer backbone. The presence of a TiO<sub>2</sub> peak at about 500 cm<sup>-1</sup> in nanocomposites indicates that TiO<sub>2</sub> has successfully interacted with polythiophene. It is worth noting that the presence of polythiophene and TiO<sub>2</sub> peaks in polythiophene/TiO<sub>2</sub> nanocomposite indicate the presence of both compounds in the nanocomposite (5). The FT-IR for polythiophene/ZrO<sub>2</sub> nanocomposite is shown in Fig. 3. Absorption bands in the prepared samples are in complete agreement with the results of the previous nanocomposite. The polythiophene adsorption peak at 3416 cm<sup>-1</sup> is related to OH bending and in 1634 cm<sup>-1</sup> is related to the presence of molecular water. The absorption peak at 1052 cm<sup>-1</sup> corresponds to the Zr-O-Zr asymmetric vibrating mode(27).

Fig. 4 and 5 showed the XRD pattern of TiO<sub>2</sub> NPs, ZrO<sub>2</sub> NPs, and pure polythiophene as the raw materials and prepared nanocomposites. The XRD pattern of TiO<sub>2</sub> NPs has various sharp peaks confirmed that the NPs has a crystalline structure. By observing the XRD pattern of pure polythiophene, it can be seen that a broad peak is obtained at about 10-30 degrees, indicating the presence of an amorphous and non-crystalline polythiophene structure. It was confirmed that the nanocomposite has a very weak crystalline structure. On the other hand, the XRD pattern for polythiophene/TiO<sub>2</sub> is considered a tetragonal crystalline structure due to the dominant structure of amorphous in the nanocomposite (5). The results for the prepared nanocomposites indicate that there is a physical combination between the nanocomposite components and the heterogeneous properties of the solid mixture. According to previous studies, it can be stated that XRD nanocrystals are covered by a polythiophene matrix, and TiO<sub>2</sub> acts

as a core and such coating causes particles of a small size to be synthesized from the nanocomposite formed by the polymerization process (14). The main peak of the polythiophene/TiO<sub>2</sub> nanocomposite is similar to that of TiO<sub>2</sub> NPs, which is related to the crystalline structure of TiO<sub>2</sub> in the polythiophene/TiO<sub>2</sub> nanocomposite coated with polythiophene. Due to the fact that the polythiophene peak still exists but its severity declined, the results indicate that TiO<sub>2</sub> has not been effective in the crystalline structure of the polythiophene (19). The XRD pattern for polythiophene/ZrO<sub>2</sub> nanocomposite was shown in Fig. 5. The result for this nanocomposite is almost the same. In general, it can be admitted that the presence of NPs is very important for the polymorphism of polythiophene.

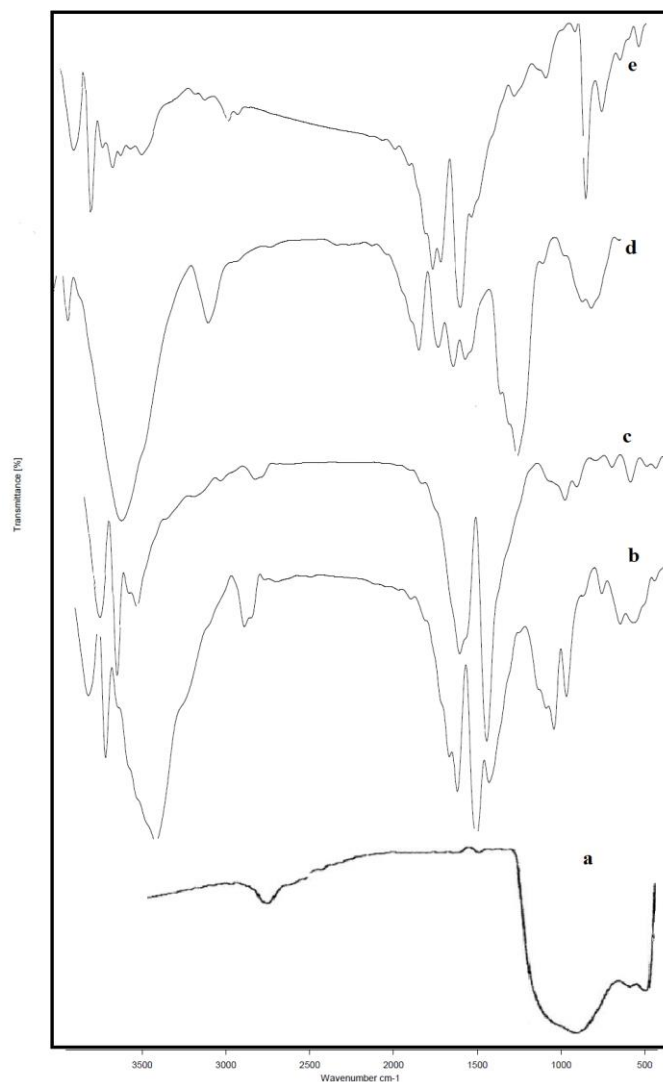


**Fig. 2.** FT-IR spectra of TiO<sub>2</sub> (a), polythiophene (b), polythiophene/TiO<sub>2</sub> nanocomposite 0.05 (c), 0.10 (d), and 0.20 (e).

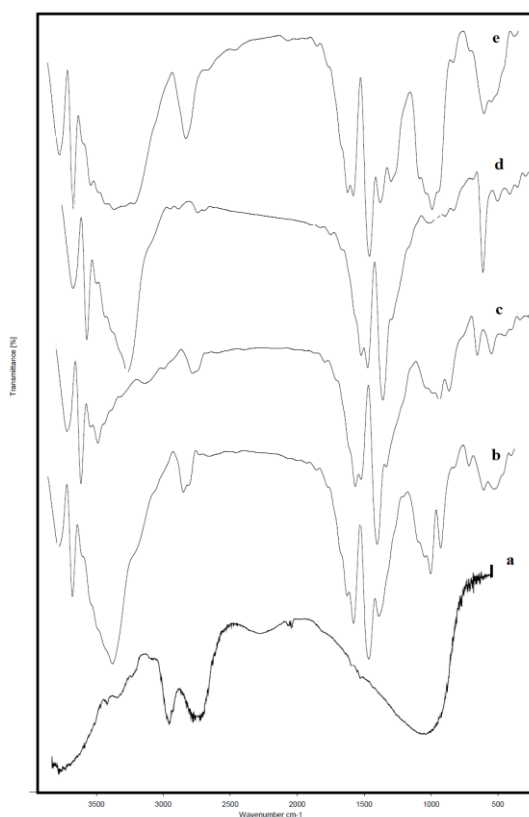


Fig. 3. FT-IR spectra of ZrO<sub>2</sub> (a), polythiophene (b), polythiophene/ZrO<sub>2</sub> nanocomposite 0.05 (c), 0.10 (d), and 0.20 (e).

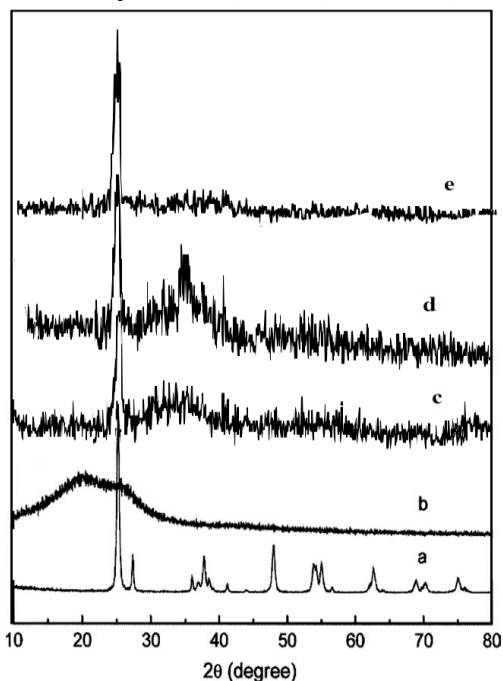


Fig. 4. XRD pattern of TiO<sub>2</sub> (a), polythiophene (b), polythiophene/TiO<sub>2</sub> nanocomposites 0.05 (c), 0.1 (d), and 0.2 (e).

Fig. 5 showed the TGA/DAT curve of the prepared polythiophene/TiO<sub>2</sub> nanocomposite. Polythiophene/TiO<sub>2</sub> nanocomposite has two stages of thermal degradation which the first degradation temperature of the nanocomposite appeared at 262 °C. According to the TGA analysis, the second structural degradation was around 601 °C. The residual polythiophene nanocomposite was completely degraded at above 650 °C. The first degradation temperature depends on the interactions of polythiophene and the materials which used to make the nanocomposite.

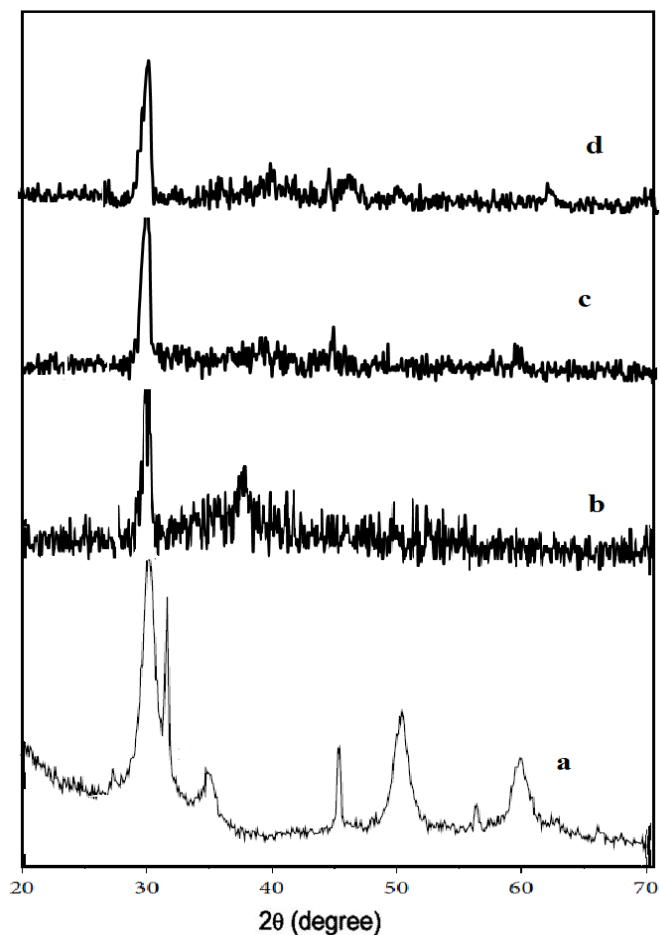


Fig. 5. XRD pattern of ZrO<sub>2</sub> (a), polythiophene (b), polythiophene/ZrO<sub>2</sub> nanocomposites 0.05 (c), 0.1 (d), and 0.2 (e).

TGA/DAT curve of the prepared polythiophene/ZrO<sub>2</sub> nanocomposite was illustrated in Fig. 7. Polythiophene/ZrO<sub>2</sub> nanocomposite has also two stages of thermal degradation; the first degradation temperature of the nanocomposite structure appeared at 250°C. According to the TGA analysis, the second structural degradation is around 550 °C. The residual polythiophene is completely destroyed in the nanocomposite above 600°C. It is observed that the degradation temperature of the polythiophene/ZrO<sub>2</sub> nanocomposite is less than that of the polythiophene/TiO<sub>2</sub> nanocomposite.

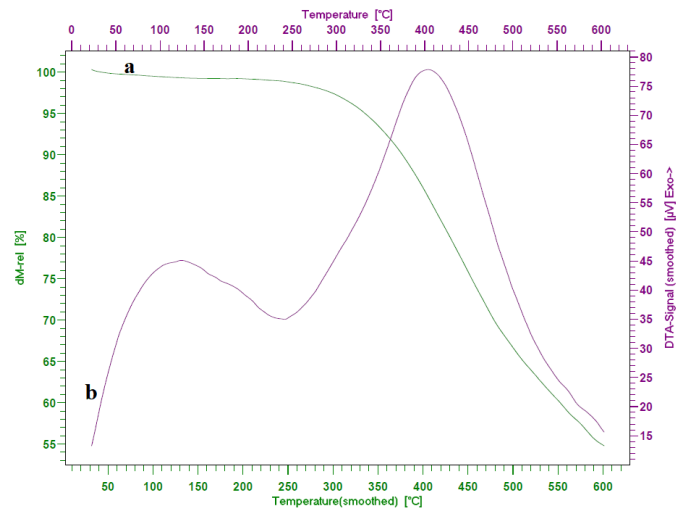


Fig. 6. DTA (a) and TGA (b) thermograms of polythiophene/TiO<sub>2</sub> 0.2.

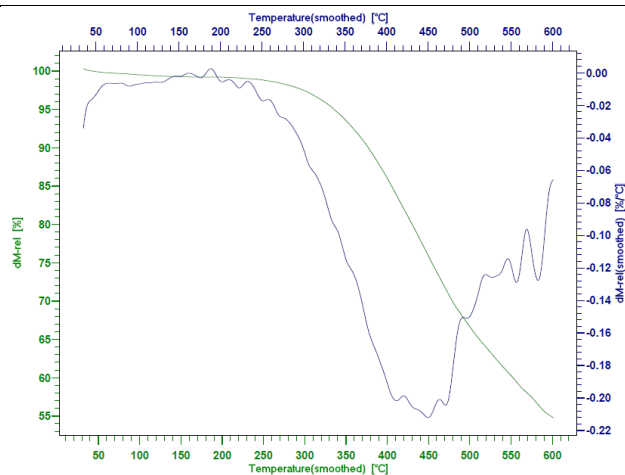


Fig. 7. DTA (a) and TGA (b) thermograms of polythiophene/ZrO<sub>2</sub> 0.2.

SEM images of polythiophene/TiO<sub>2</sub> and polythiophene/ZrO<sub>2</sub> nanocomposites are shown in Figs. 7 and 8, respectively. SEM images for polymers show that the distribution of particles in terms of their size is almost uniform. It is expected that there will be accumulation and density between nanocomposite particles. The SEM results are according to the XRD pattern results. As for the SEM image, it can be seen that the nanocomposite is integrated.

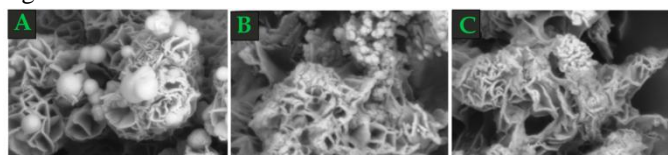


Fig. 8 SEM images of polythiophene/TiO<sub>2</sub> nanocomposites with 0.5 (A), 0.1 (B), and 0.2 (C) of NPs.

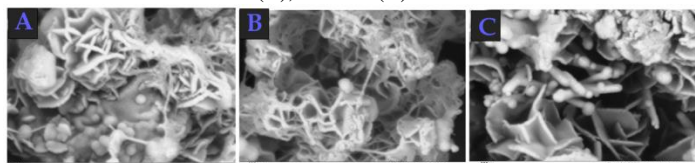


Fig. 9. SEM images of polythiophene/ZrO<sub>2</sub> nanocomposites with 0.5 (A), 0.1 (B), and 0.2 (C) of NPs.

#### 4. CONCLUSIONS

In the case of polythiophene /TiO<sub>2</sub> nanocomposites, a stable polymer structure is obtained in return for a complete correlation between nanoparticles. The high density of nanoparticles in the structure of dense nanocomposites is clearly visible through SEM images. The SEM results confirm the XRD results. The TGA/DAT curve shows that the polythiophene/TiO<sub>2</sub> nanocomposite exhibits more thermal strength than the

#### 5. REFERENCES

[1] Habibi M.H., Karimi B., Fabrication and Characterization of CuO-ZnO-Cu<sub>2</sub>O Nano-Composites by Sol-Gel Route: Effect of Calcinations Temperature Synth. React. Fa. Inorg. Met., 44, 1358–1362, **2014**.  
 [2] Bharti A., Mulianteezhu S., Cheruvally G., Pt-TiO<sub>2</sub> Nanocomposites as Catalysts for Proton Exchange Membrane Fuel Cell: Prominent Effects of Synthesis Medium pH, Journal of Nanoscience and Nanotechnology, 18, 4, 2781-2789, **2018**.  
 [3] Chen J., Wang N., Ma H., Zhu J., Feng J., Yan W., Facile Modification of a Polythiophene/TiO<sub>2</sub> Composite Using Surfactants in an Aqueous Medium for an Enhanced Pb(II) Adsorption and Mechanism Investigation, J. Chem. Eng. Data, 62, 7, 2208–2221, **2017**.

#### 3.3. Antimicrobial activity by disc diffusion method.

Antibacterial properties of prepared nanocomposites were evaluated against three different microbial strains including *E.coli*, *S.aureus*, and *C.albicans* (Fig. 10). Firstly, both nanocomposites antimicrobial activity were investigated against *E.coli* as Gram-positive bacteria which for polythiophene/TiO<sub>2</sub> was 13±2mm and polythiophene/ZrO<sub>2</sub> was 10±1mm. The results indicated that the polythiophene/TiO<sub>2</sub> nanocomposite had a more antibacterial effect. Antimicrobial properties against *S. aureus* was 8±1mm for polythiophene/TiO<sub>2</sub> and 9±1 mm for polythiophene/ZrO<sub>2</sub>. These results indicate polythiophene/ZrO<sub>2</sub> had more activity against gram positives. Antimicrobial activity against *C. albicans* was 7±1mm for polythiophene/TiO<sub>2</sub> and 6±1 mm for polythiophene/ZrO<sub>2</sub>. Both of nanocomposites had less activity against candida compared with bacterial pathogens. These results indicate better activity for polythiophene/TiO<sub>2</sub> in comparison with polythiophene/ZrO<sub>2</sub> against gram negatives and their potential for control of infections, especially in burn patients at risk of gram-negative infections.

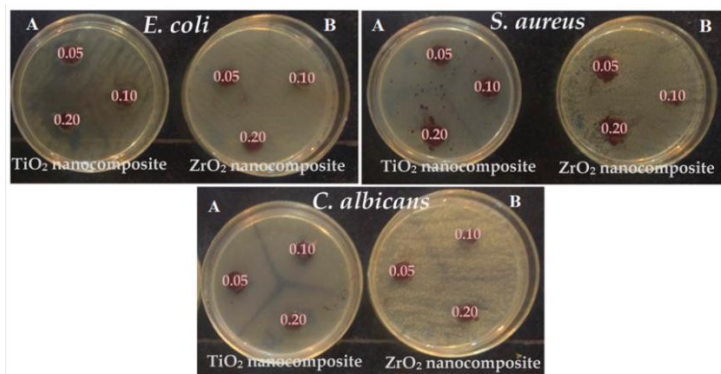


Fig. 10. Antimicrobial activity of prepared nanocomposites against *E. coli*, *S.aureus*, and *C. albicans*: polythiophene/TiO<sub>2</sub> (A) and polythiophene/ZrO<sub>2</sub> (B) with various amounts of NPs (0.05, 0.10, and 0.20).

polythiophene/ZrO<sub>2</sub> nanocomposite. Also, polythiophene/TiO<sub>2</sub> nanocomposite had higher antibacterial properties compared to polythiophene/ZrO<sub>2</sub> against *E.coli* bacteria, but polythiophene/ZrO<sub>2</sub> nanocomposite had a better effect against *S. aureus*. In addition, the two nanocomposites prepared in this study had less antifungal activity compared with their antibacterial properties.

[4] Mehrabani M.G., Karimian R., Mehramouz B., Rahimi M., Kafil H.S., Preparation of biocompatible and biodegradable silk fibroin/chitin/silver nanoparticles 3D scaffolds as a bandage for antimicrobial wound dressing, Int J Biol Macromol., 114, 961-971, **2018**.  
 [5] Lu Q., Zhou. Y., Synthesis of mesoporous polythiophene/MnO<sub>2</sub> nanocomposite and its enhanced pseudocapacitive properties, J. Power Sources, 196, 4088–4094, **2011**.  
 [6] Karch J., Birringer R., Gleiter H., Ceramics ductile at low temperature, Nature, 330, 6148, 556–558, **1987**.  
 [7] Mehrabani M.G., Karimian R., Rakhshaei R., Pakdel F., Eslami H., Fakhzadeh V., Rahimi M., Salehi R., Kafil H.S., Chitin/silk fibroin/TiO<sub>2</sub>

bio-nanocomposite as a biocompatible wound dressing bandage with strong antimicrobial activity, *Int J Biol Macromol*, 116, 966-976, **2018**.

[8] Hirvonen A., Nowak R., Yamamoto Y., Sekino T., Niihara K., Fabrication, structure, mechanical and thermal properties of zirconia-based ceramic nanocomposites, *Journal of the European Ceramic Society*, 26, 8, 1497–1505, **2006**.

[9] Roy S., Nanocrystalline undoped tetragonal and cubic zirconia synthesized using poly-acrylamide as gel and matrix, *Journal of Sol-Gel Science and Technology*, 44, 3, 227–233, **2007**.

[10] Ates M., Dolapdere A., Electrochemical polymerization of Thiophene and poly(3-hexyl)thiophene, *Nanocomposites with TiO<sub>2</sub>, and Corrosion protection behaviours*, *Polymer-Plastics Technology and Engineering*, **2015**.

[11] Namazi H., Rakhshaei R., Hamishehkar H., Kafi H.S., Antibiotic loaded carboxymethylcellulose/MCM-41 nanocomposite hydrogel films as potential wound dressing, *Int J Biol Macromol*, 85, 327-34, **2016**.

[12] Wright P.K., Evans A.G., Mechanisms governing the performance of thermal barrier coating, *Current Opinion in Solid State and Materials Science*, 4, 25–30, **1999**.

[13] Zeynabad F.B., Salehi R., Alizadeh E., Kafil H.S., Hassanzadeh A., Mahkam M., pH-Controlled multiple-drug delivery by a novel antibacterial nanocomposite for combination therapy, *RSC advances*, 5, 128, 105678-105691, **2015**.

[14] Kumari L., Du G. H., Li W.Z., Vennila R.S., Saxena S.K., Wang D.Z., Synthesis, microstructure and optical characterization of zirconium oxide nanostructures, *Ceramics International*, 35, 6, 2401–2408, **2009**.

[15] Park S., Vohs J. M., Gorte R.J., Direct oxidation of hydrocarbons in a solid-oxide fuel cell, *Nature*, 404, 6775, 265–267, **2000**.

[16] Salas P., de la Rosa-Cruz E., Diaz-Torres L.A., Castaño V.M., Meléndrez R., Barboza-Flores M., Monoclinic ZrO<sub>2</sub> as a broad spectral response thermoluminescence UV dosimeter, *Radiation Measurements*, 37, 2, 187–190, **2003**.

[17] Guo H., Liu L., Shu H., Yang X., Yang Z., Zhou M., Tan J., Yan Z., Hu H., Wang X., Synthesis and electrochemical performance of LiV<sub>3</sub>O<sub>8</sub>/polythiophene composite as cathode materials for lithium ion batteries, *J. Power Sources*, 247, 117–126, **2014**.

[18] Huang J., Kang Y., Yang T., Wang Y., Wang S., Preparation of polythiophene/WO<sub>3</sub> organic-inorganic hybrids and their gas sensing properties for NO<sub>2</sub> detection at low temperature, *J. Nat. Gas Chem.*, 20, 403407-, **2011**.

[19] Zhu Y., Xu S., Yi D., Photocatalytic degradation of methyl orange using polythiophene/titanium dioxide composites, *React. Funct. Polym*, 70, 282–287, **2010**.

[20] Dongmei L., Wen Z., Ming L., Changqing X., Chengcheng H., Xing W., Xuefeng Y., Institute of Microelectronics of Chinese Academy of Sciences, assignee. Making method of polythiophene-zirconia composite sensitive membrane, CN patent, **2013**.

[21] Ziane B., Chaib M., Badaoui M. Photocatalytic decolorization of indigo-carmin dye by sol-gel synthesized doped ZrO<sub>2</sub> photocatalyst. *Biointerface Research in Applied Chemistry*, 7, 2, 1998-2003, **2018**.

[22] Topel SD, Topel Ö, Cin GT. Fabrication and characterization of TiO<sub>2</sub> nanoparticles conjugated luminescence upconversion nanoparticles. *Biointerface Research in Applied Chemistry*, 8, 3, 3197-202, **2018**.

[23] Hatamzadeh M., Jaymand M., Synthesis and characterization of polystyrene-graft-polythiophene via a combination of atom transfer radical polymerization and Grignard reaction, *RSC Advances*, 4, 32, 16792-16802, **2014**.

[24] Wayne P.A., CLSI, Performance Standards for Antimicrobial Susceptibility Testing. 27th ed. CLSI supplement M100.; Clinical and Laboratory Standards Institute, **2016**.

[25] Aghazadeh M., Zahedi Bialvaei A., Kabiri F., Saliyani N., Yousefi M., Eslami H., Samadi Kafil H., Survey of the Antibiofilm and Antimicrobial Effects of Zingiber officinale (in Vitro Study), *Jundishapur J Microbiol*, 9, 2, **2016**.

[26] Kafil H.S., Mobarez A.M., Moghadam M.F., Hashemi Z.S., Yousefi M. Gentamicin induces efaA expression and biofilm formation in *Enterococcus faecalis*. *Microb Pathog*. 92, 30-5, **2016**.

[27] Ray J.C., Park D., Ahn W., Chemical synthesis of stabilized nanocrystalline zirconia powders, *Journal of Industrial and Engineering Chemistry*, 12, 1, 142–148, **2006**.